Transactions of the 15th International Conference on
Structural Mechanics in Reactor Technology (SMiRT-15)
Seoul, Korea, August 15-20, 1999

Stability of Rubber Bearings for Seismic Isolation

Jong Seh Lee and Jong Won Oh

Hanyang University, Korea

ABSTRACT

Laminated rubber bearings(LRB's) are widely used as a basic component in seismic isolation systems for structures. Increasing the number of steel shims and thickness of the elastomers can achieve large period shifts. However, the shear flexibility of these short columns can lead to relatively low buckling loads which may be further reduced when high shear strains are applied. In this paper, a nonlinear finite element study is presented with an aims at determining the effect of high shear strain on the critical load of elastomeric bearings. Both the geometric and material nonlinearities are considered in the study. From the load-displacement curve for each specified shear displacement, the buckling load is calculated using the Southwell procedures. The results obtained are then compared against the theoretical predictions in order to examine the validity and the conservatism of the theoretical formulas.

INTRODUCTION

Recent surveys of seismic isolation systems around the world indicate that the majority of these systems use elastomeric bearings as the element of flexibility. These bearings may be of natural or synthetic rubber and usually compounded to enhance their hysteretic damping. These typically consist of several layers of rubber inter-layered by steel shims. This composite structure results in a very high vertical stiffness without a considerable increase in the horizontal stiffness over the same rubber block lacking reinforcement. In a typical building, isolators are located under each column, usually in a sub-basement. In a bridge they may be placed under each girder at the abutment seats and between the column capbeam and the superstructure. The individual bearings which make up the isolation systems are frequently interconnected by a diaphram which is rigid in its own plane and enforces displacement compatibility amongst the various isolators.

Of particular interest to the design engineer is the failure modes or limit states of the isolator systems. There are three separate limit states to consider. These are the maximum shear strain in the rubber compound, the displacement at which roll-over commences, and the load at which buckling occur. This paper is concerned with the buckling limit state of laminated elastomeric bearings under the combined actions of compression and shear. Although it is recognized that the system stability

is a function of the spatial distribution of axial load and bearing stiffness, the properties of individual bearings must be well understood in order to make meaningful calculations of system response.

STABILITY THEORY OF RUBBER BEARINGS

Laminated elastomeric bearings exhibit buckling phenomena in much the same way that structural columns are susceptible to compressive loads. Despite their short length, these columns may have low critical loads due to their extreme flexibility in shear compared with steel bearings. Associated with the buckling phenomenon is the corresponding dependence of shear stiffness on axial loads. The relationship between axial load and shear stiffness at small shear deformations has been established. The theory for the buckling of isolation bearings is an outgrowth of work by Haringx[1] on the mechanical characteristics of helical steel springs and rubber rods used for vibration mountings. The Haringx theory was later applied by Gent[2,3] to the problem of the stability of multilayer rubber springs. Gent's extension forms the basis of the stability theory given below[4].

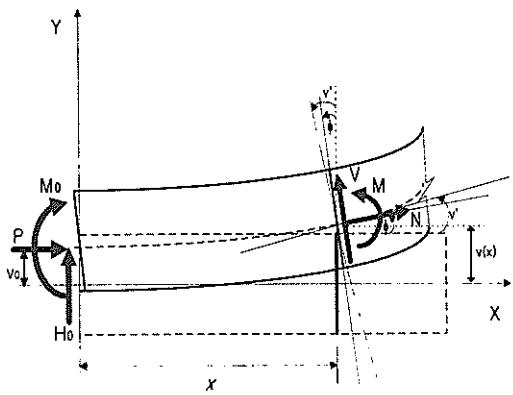

Fig. 1 Internal forces and external loads on a deformed bearing

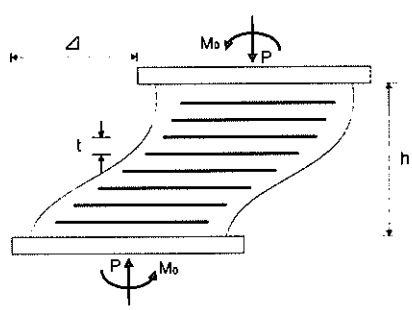

Fig. 2 Boundary conditions

Fig. 1 shows the internal and external forces on the bearing in the deformed position. The equations of equilibrium for bending moment and shear force in the deformed state are given by

$$M+P(v-v_0)-M_0-H_0x=0 \tag{1}$$

$$V+H_0-P\psi=0 \tag{2}$$

where v(x) is the displacement of the middle surface of the bearing and $\psi(x)$ is the rotation of the face originally normal to the undeformed axis. P, M and, M_0 are the axial load, lateral reaction, and bending moments, respectively.

Upon substitution of the constitutive equations and applcation of the boundary conditions shown in Fig. 2, the solution for v(x) and $\psi(x)$ can be given by the following:

$$v(x)=\frac{1}{2}\left(1-\cos\frac{\pi x}{h}\right)v(h) \tag{3}$$

$$\psi(x)=\frac{1}{2}\frac{\alpha(GA)_{eff}}{(GA)_{eff}+P}\left(\sin\frac{\pi x}{h}\right)v(h) \tag{4}$$

where

$$\alpha^2=\frac{P((GA)_{eff}+P)}{(EI)_{eff}\cdot(GA)_{eff}}=\frac{\pi^2}{h^2} \tag{5}$$

From the above equations, the buckling load P_{cr} can be determined as the followings:

$$P_{cr}=\frac{(GA)_{eff}}{2}\left[\left(1+\frac{4P_E}{(GA)_{eff}}\right)^{\frac{1}{2}}-1\right] \tag{6}$$

where

$$P_E=\frac{\pi^2(EI)_{eff}}{h^2}=\text{Euler buckling load}$$

$$(EI)_{eff}=\frac{4S^2}{15}EI\left(\frac{h}{t}\right)=\text{Effective bending stiffness}$$

$$(GA)_{eff}=GA\left(\frac{h}{t}\right)=\text{Effective shear stiffness}$$

In the above, EI and GA denote the bending and shear stiffness respectively; S is the shape factor defined by b/t; b and h are the half-width and height of the bearing respectively; t is the thickness of the thickness of a single rubber layer. The buckling theory described above, however, is applicable only to the bearings at zero shear displacement. Various approximate methods have been proposed to account for the reduction in buckling load when there are non-zoro shear displacements as

shown in Fig. 3. The most common method is the area reduction formula given by Eq. (7) which implies that the critical load is zero when the shear displacement is equal to the width of the bearing[5].

$$\overline{P_{cr}} = P_{cr}\left(1 - \frac{\Delta}{B}\right) \tag{7}$$

where $\overline{P_{cr}}$ is the modified buckling load, P_{cr} the buckling load calculated by Eq. (6), B the bearing width, and Δ the shear displacement. The validity of the formula is also to be examined in this study.

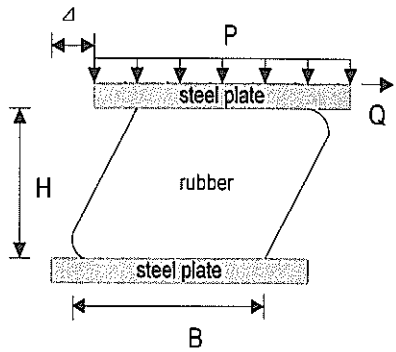

Fig. 3 Elastomeric bearing under combined compression and shear

FINITE ELEMENT ANALYSIS

The objective of the finite element analysis is to examine the buckling behavior of elastomeric bearings with high shear strains. Critical loads at imposed shear strains are determined using the Southwell Plot method[6]. As a finite element analysis program, the LUSAS[7] computer program is chosen. This program permits the geometric and material non-linearities of both compressible and almost incompressible solids. Incremental analysis is performed using a displacementbased finite element formulation. The Mooney-Rivlin material model is used to characterize the rubber at high strains, and the co-rotational formulation to address the geometric non-linearity. A hydrostatic work term was added to the energy function to permit the inclusion of compressibility in the rubber. In order to reduce the computational effort, a plane strain restriction is imposed so that 2-D analyses could be performed. This assumption is valid for strip elastomeric bearings, but care should be taken when applying these results to square or rectangular bearings.

Table 1 summarizes the three bearings analyzed. They are all 12 cm wide and 10 cm tall with the number of internal layers to be three, four or five. The shape factor ranges from 3.75 to 6.67 which is considered to be important in a comparative study of buckling loads.

Table 1. Bearing details Unit: cm

Series No.	Width	Height	No. of Rubber Layer	Thickness of Rubber Layer	Shape Factor
LRB1	12	10	3	1.6	3.75
LRB2	12	10	4	1.15	5.22
LRB3	12	10	5	0.9	6.67

In the case of LRB2 model, the finite element mesh with 4 layers comprised of 1000 elements, 1074 nodes and 2148 displacement degrees of freedom. Fig. 4 and 5 show the dimensions of the bearing and the corresponding finite element mesh respectively.

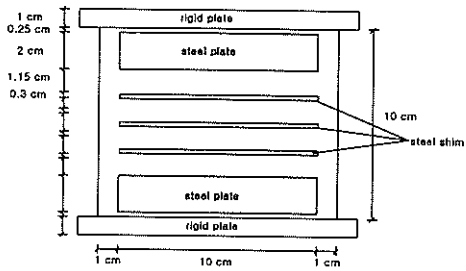

Fig. 4 Dimensions of Bearing (LRB2)

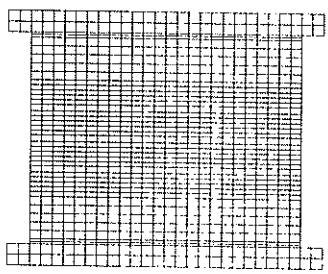

Fig. 5 FE Model (LRB2)

The bearings are first deformed in shear to a predetermined lateral displacement (Δ) and the additional lateral displacement (δ) is monitored as the axial load (P) is increased. Figs. 6(a) and (b) show the deformed finite element meshes which are first loaded in shear and then deformed in compression respectively. It can be seen in the figures that the steel reinforcements experience very little deformation compared to the rubber elements.

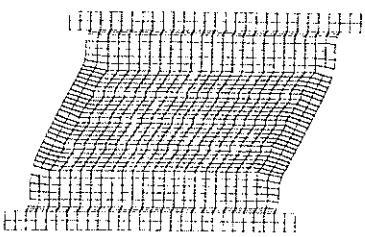

(a) Shear Only

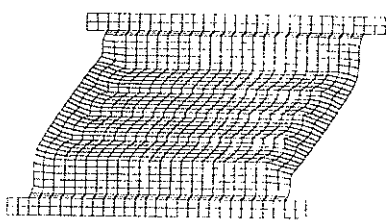

(b) Compression After Shear

Fig. 6 Deformed Mesh (LRB2)

NUMERICAL RESULTS

Lateral displacements described above are plotted against the vertical loads for

each specified shear displacement in Fig. 7. The Southwell Plot may be applied to each P - δ curve in Fig. 7 to determine the buckling load for the specified shear displacement. In the Southwell procedure, the ratio P/Δ is plotted against P, and a straight line is then fitted to the calculate responses. The intercept of this line with the horizontal axis is an indicator of the critical load at the specified initial displacement Δ. An example is shown in Fig. 8 where the apparent critical load is determined to be 730 KN at the initial displacement of 3 cm.

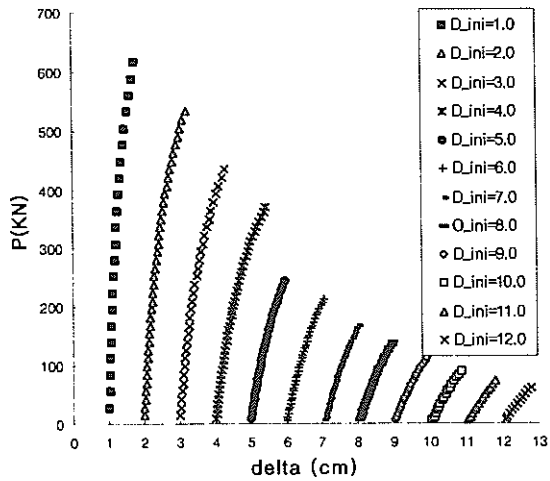

Fig. 7 P - δ Plot (LRB2)

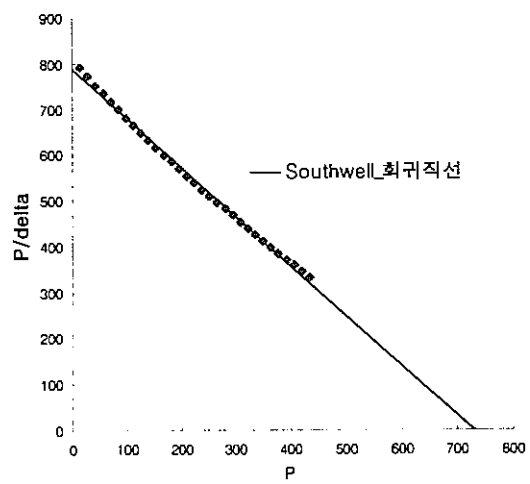

Fig. 8 Southwell Plot (Δ=3cm, LRB2)

Fig. 9 shows the bucking load as a function of the shape factor. It can be seen that the critical loads from the finite element analysis become smaller than the theoretical predictions when shape factors are greater than about 5.

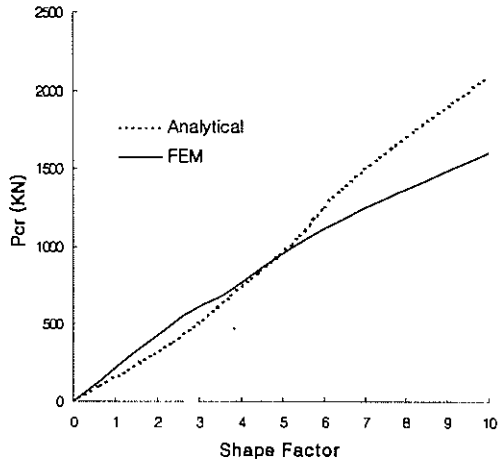

Fig. 9 Bucking loads for different shape factors

The effective buckling load ratio($\overline{P_{cr}}/P_{cr}$) is plotted against the shear displacement as a fraction of the bearing width in Fig. 10. Also shown in Fig. 10 is the relationship given by Eq. (7) for comparison. It is shown in the figure that the numerical results start to veer from the straight line when the shear displacement is about 40 percents of the bearing width. Fig. 10 indicates a substantial residual capacity at Δ = B whereas Eq. (7) implies that $\overline{P_{cr}}$ should be zero at this point.

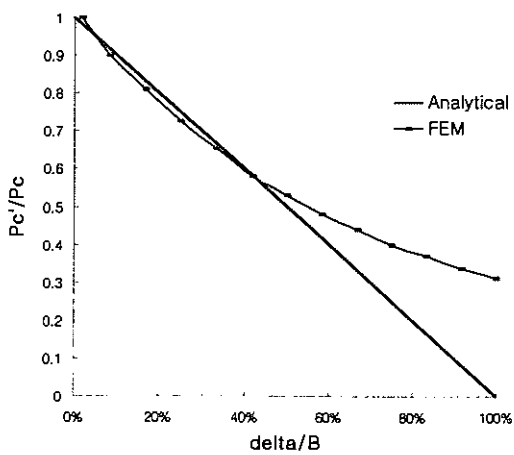

Fig. 10 Effective buckling load ratio (Δ=3cm, LRB2)

CONCLUSIONS

A finite element analytical study is carried out to determine the buckling loads of laminated rubber bearings with an aim at developing a viable numerical technique for critical load analysis of isolation bearings. From the results of the limited number of cases considered, it appears that a substantial reserve of the vertical load capacity exists even after the shear displacement reaches way about 40 percents of the bearing width. It may be calculated that the area reduction formula is a conservative estimate of the reduction in critical load due to the effective of high shear strains. Since there is some degree of restraint in most bearing isolation systems the unrestrained results may be more conservative. Additional case studies should be performed to determine if this is generally true.

ACKNOWLEDGEMENT

This work was supported in part by the Korea Science and Engineering Foundation(KOSEF) through the Korea Earthquake Engineering Research Center at Seoul National University.

REFERENCES

1. Haringx, J. A., "On Highly Compressible Helical Springs and Rubber Rods, And Their Application For Vibration-Free Mountings II," *Philips Res. Report* 4, pp.49~80, 1948

2. Gent, A. N. and Lindley, P. B., "The Compression of Bonded Rubber Blocks," *Proc. Instn. Mech. Engrs*, Vol. 173, No 3., pp.111~117, 1959

3. Gent, A. N., "Elastic Stability of Rubber Compression Springs," *Journal of Mechanical Engineering Sciences*, Vol.6, No. 4, pp. 318~326, 1964

4. Kelly, J. M., *"Earthquake-Resistant Design with Rubber,"* 2nd Ed., Springer-Verlag, London, England, 1997

5. Buckle, I. G., and Liu, He., "Finite Element Analysis of Elastomeric Isolation Bearings for different Connection Details," *Proceedings from the First U.S.-Japan Workshop on Earthquake Protective Systems for Bridges*, Technical Report NCEER-92-0004, pp.151~167, 1992

6. Koh, C. G., and Kelly, J. M., "Applicability of the Southwell Plot to Shear Deformable Columns," *Journal of Testing and Evaluation*, Vol. 17, No. 5, pp.287~291, 1989

7. FEA Ltd., *"LUSAS Element Library, User's Guide, Theory Manual,"* Ver. 12, London, England, 1997